Next-to-Leading Order QCD Corrections to the Production of Two Bottom-Antibottom Pairs at the LHC

Nicolas Greiner, Alberto Guffanti, Thomas Reiter, and Jürgen Reuter

NLO QCD corrections to the production of two bottom-antibottom pairs at the LHC

Nicolas Greiner,[1] Alberto Guffanti,[2] Thomas Reiter,[3, 4] and Jürgen Reuter[5, 2]

[1]*Department of Physics, University of Illinois at Urbana-Champaign, Urbana IL, 61801, USA*
[2]*Physikalisches Institut, Albert-Ludwigs-Universität, 79104 Freiburg, Germany*
[3]*Nikhef, 1098 XG Amsterdam, The Netherlands*
[4]*Max-Planck-Institut für Physik, 80805 München, Germany*
[5]*DESY, 22607 Hamburg, Germany*
(Dated: July 29, 2011)

We report the results of a computation of the full next-to-leading order QCD corrections to the production of two $b\bar{b}$ pairs at the LHC. This calculation at the parton level provides predictions for well separated b-jets. The results show that the next-to-leading order corrections lead to an enhancement of the cross-section for the central scale choice by roughly 50% with respect to the leading order result. The theoretical uncertainty estimated by variation of the renormalization and factorization scales is strongly reduced by the inclusion of next-to-leading order corrections.

PACS numbers: 12.38.Bx, 13.85.Hd, 14.65.Fy

INTRODUCTION

The search for the Higgs boson, and more in general the study of the Electroweak Symmetry breaking mechanism, is a major goal of the experiments at the LHC collider at CERN. In various extensions of the Standard Model the signature of two light Higgs bosons decaying in two pairs of b-quarks, $hh \to b\bar{b}b\bar{b}$, is a viable channel for the Higgs Boson discovery. Examples of these models are the Minimally Supersymmetric Standard Model (MSSM) for large values of $\tan\beta$ and moderate m_A [1–4], hidden valley scenarios where the decay of hadrons of an additional gauge group can produce additional b-jets [5, 6] and two Higgs doublet models. The possibility of measuring the Higgs self-coupling through $H \to hh \to b\bar{b}b\bar{b}$ has been investigated in [7]. This and other related studies, however show that such a measurement would be extremely difficult, primarily due to the large Standard Model background. The precise knowledge of the $b\bar{b}b\bar{b}$ final state within the Standard Model is therefore an important factor for the success of these measurements.

Because of its importance this process has been added to the Les Houches wish list of relevant next-to-leading order calculations [5].

In an earlier publication [8], we presented the next-to-leading order (NLO) QCD corrections to the production of $b\bar{b}b\bar{b}$ via quark-antiquark annihilation. In the present Letter we complete the existing work including the gluon initiated contributions and present the results for the full NLO QCD corrections to $pp \to b\bar{b}b\bar{b}$ at the LHC.

We show that the inclusion of the NLO corrections reduces the unphysical scale dependence of the leading order (LO) prediction greatly, improving the precision of this prediction and allowing a better estimation of the Standard Model background to possible New Physics signals in this channel.

METHOD

A complete NLO QCD description requires the calculation of the $2 \to 4$ subprocesses $q\bar{q} \to b\bar{b}b\bar{b}$ and $gg \to b\bar{b}b\bar{b}$ at the tree and the one-loop level as well as the $2 \to 5$ particle processes $q\bar{q} \to b\bar{b}b\bar{b}g$, $gg \to b\bar{b}b\bar{b}g$ and $\overset{(-)}{q}g \to b\bar{b}b\bar{b}\,\overset{(-)}{q}$ at tree level.

We sum over four massless quark flavours $q \in \{u, d, s, c\}$ in the initial state. Neglecting the contribution from initial state b-quarks is justified by the smallness of the b parton distribution function (PDF) with respect to the other quark PDFs. Moreover the fact that the gluon-gluon channel is the dominant contribution at LHC energies further reduces the relative importance of the quark channels. We treat the b-quarks as massless, which is a very good approximation for LHC kinematics also due to the cuts imposed in order for the final state b-quarks to be detected and separated in phase space. Effects of the heavy top quark are neglected altogether in the final result after having shown that they are numerically not important.

The LO and the real radiation matrix elements are generated using MadGraph [9]. For the subtraction of the infrared singularities we use Catani-Seymour dipoles [10], supplemented with a slicing parameter α as proposed in [11, 12], implemented in the MadDipole package [13, 14].

As described in our earlier work [8], we compute the one loop corrections to scattering matrix elements using an approach based on Feynman diagrams. The code for the numerical evaluation of the virtual corrections is generated using an extension [15] of the automated one-loop matrix element generator `golem-2.0` [16–18] which employs QGraf [19], Form [20], the Form library Spinney [21] and the code generator Haggies [22] at intermediate levels of the diagram and code generation, that has been upgraded to the production of numerators to be reduced through modern reduction algorithms [23–26]. The evaluation of the loop integrals is performed using OneLOop [27].

The integration over phase space is carried out using MadEvent [28] and it has been split up in independent parts in order to optimize the computational time required.

The first contribution consists of the real emission matrix element supplemented with the subtraction terms. The integration of this contribution over the corresponding 13-dimensional phase space is one of the main computational bottlenecks of such a calculation. This integration has been performed using up to $2 \cdot 10^9$ phase space points. For the $q\bar{q}$ and gg subprocess the evaluation of a single phase space point requires the evaluation of 30 subtraction terms for each partonic channel and an additional 10 subtraction terms are needed for the qg channel. This means that a substantial fraction of CPU time is spent calculating the dipole contributions. In such a situation the use of a value smaller than one for the slicing parameter α, as proposed in [11, 12]. The use of a slicing parameter $\alpha < 1$ effectively restricts the phase space volume of the dipole evaluation to the vicinity of the singular regions thus speeding up substantially the computation by avoiding that each subtraction term is evaluated for each phase-space point. Besides the reduction of the computational time per point this setting has a second advantage. If not close to a singularity the integrand

is given just by the real emission matrix element. Close to a singularity, where also subtraction terms are calculated, these subtraction terms per definition have the same kinematical structure as the real emission matrix element which is not necessarily true for an arbitrary point in phase space. So for each point the integrand is either exactly the real emission matrix element or something with the same structure but with one singularity subtracted. But as this is an integrand where our integration routine is optimized for, choosing a value for α smaller than one leads to an improvement of the convergence of the integral. In our calculation we set $\alpha = 0.01$.

The second contribution to the integration combines the tree-level contribution and the integrated subtraction terms. The virtual matrix element is integrated over phase space by reweighting a sample unweighted Born level events, as described in [16]. This leads to a considerable reduction of the required CPU-time since less phase space points have to be evaluated. For the results shown below, event samples consisting of $10^4 - 10^5$ unweighted events have been used. The LO event samples used for the reweighting have been generated with MadEvent [28] and WHIZARD [29, 30].

In order to establish the correctness of the results obtained we have performed a number of non-trivial tests. The dipole contributions for single phase space points and at the phase space integration level have been compared with the HELAC code [31, 32] and agreement has been established up to double precision accuracy for single phase space points and within integration errors for the integrated results. The phase space integration of the dipole contributions is validated by checking the independence of the result of the slicing parameter α. Also the cancellation of the single and double poles between the virtual amplitude and the integrated subtraction terms has been verified. Finally, the virtual matrix element computation for a single phase space point has been compared to the result published in [33]. In order to perform this comparison the contribution from top quark loops has been added, even though it is neglected in the results presented in the following section. Our result is in agreement with the result of [33], providing a very strong test of our virtual contributions computations.

RESULTS

In the following we consider the process $pp \to b\bar{b}b\bar{b} + X$ at the LHC at a center of mass energy of $\sqrt{s} = 14\,\text{TeV}$. The final state jets are defined by applying the k_T-algorithm as explained in [34] with a radius in R-space of 0.8. More precisely, the jet algorithm requires exactly four b-jets in the final state for the event to be accepted. All jets are required to lie within a rapidity range of $|\eta(b_j)| < 2.5$ and to have a transverse momentum $p_T(b_j) > 30\,\text{GeV}$. We impose a separation cut between the jets of $\Delta R(b_i, b_j) = \sqrt{(\phi_i - \phi_j)^2 + (\eta_i - \eta_j)^2} > 0.8$. All results have been obtained using the CTEQ6M parton distribution functions [35] with two-loop running of α_s both for the LO and the NLO cross-section evaluations and $\alpha_s(M_Z) = 0.118$.

The unphysical renormalization and factorization scales are usually chosen to be in the vicinity of the typical scale of the process. For processes where heavy particles such as top-quarks or W/Z-bosons are involved the masses of these particles provide a natural choice. In our case, dealing with massless particles only there is no such scale, the only scale involved in this process is the p_T-cut imposed to define the b-jets. In this respect the process considered here is similar to the production of four light jets. In [12] it has been shown that the average transverse momentum p_T of a jet is a good choice for the production of three jets in hadron-hadron collisions. On the basis of the scale choice we made earlier for the quark initiated case [8], we define the central scale to be

$$\mu_0 = \tfrac{1}{4}\sqrt{\sum_i p_{T,i}^2}\,, \tag{1}$$

which turns out to be of the same order of magnitude as the average p_T of the jets.

In Figure 1 we plot the variation of the total cross section for the production of two bottom-antibottom pairs at the LHC, with the cuts described previously, when the renormalization scale μ_r and the factorization μ_F are varied together, with x defined as the ratio to the the central scale, $\mu_r = \mu_F = x \cdot \mu_0$.

If we set the renormalization and factorization scale to the value μ_0 as in Eq. (1) we find for the total cross section with the cuts described above

$$\sigma_{pp \to b\bar{b}b\bar{b}}^{NLO} = 140.48\ \pm\ 0.64\,\text{pb}\,, \tag{2}$$

where the quoted uncertainty refers to the error coming from the Monte Carlo integration over phase space. This means that for our preferred choice of scales we find that the inclusion of the NLO contribution leads to an increase of nearly 50% of the total cross section with respect to the LO result of $\sigma^{LO} = 94.88 \pm 0.14$ pb. However one observes that, as expected, the dependence of the result on the unphysical scales is strongly reduced in the NLO result with respect to the leading order one.
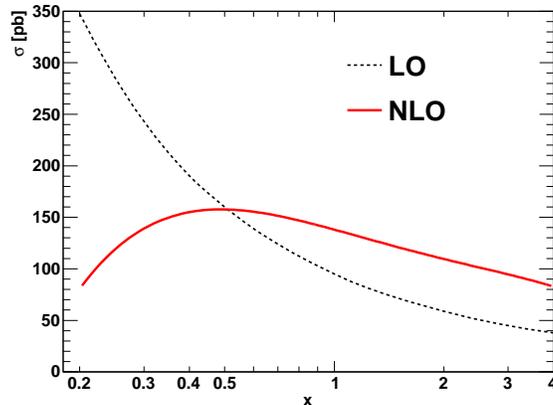
FIG. 1. Total cross section as a function of the scale $\mu = \mu_r = \mu_F = x \cdot \mu_0$. Renormalization and factorization scale are varied in the same direction.
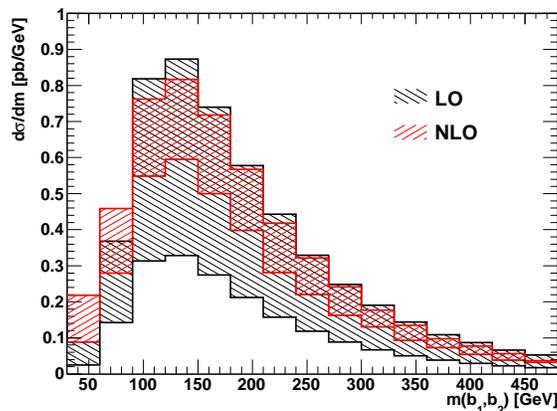

FIG. 2. Invariant mass distribution of the two b-jets with the highest p_T. The black shaded area denotes the tree level contribution, the red area denotes the NLO cross-section. The error bands for both histograms are determined by a scale variation between $\mu_0/2$ and $2\mu_0$.

In Figure 2 we plot the invariant mass distribution of the two b-jets with the highest transverse momentum. The error bands are obtained by a variation of the scales between $\mu_0/2$ and $2\mu_0$. With respect to the LO result one observes a shift of the distribution to lower energies due to the inclusion of the radiative corrections. The p_T distribution of the jet with the highest p_T is shown in Figure 3. Here, the radiative corrections enhance the distribution at higher momentum. Both Figure 2 and Figure 3 show a significant reduction of the error induced by scale uncertainties on differential distributions. Moreover, the distortion in the shapes of differential distributions when going from LO to NLO suggests that the application of a global K-factor is not sufficient in order to accurately describe the higher-order effects.

A complete phenomenological study of the production of two bottom-antibottom pairs at the LHC, including the study of PDF uncertainties and the effects of varying the cuts on the final state b-jets is beyond the scope of the present Letter and will be the subject of an upcoming publication.
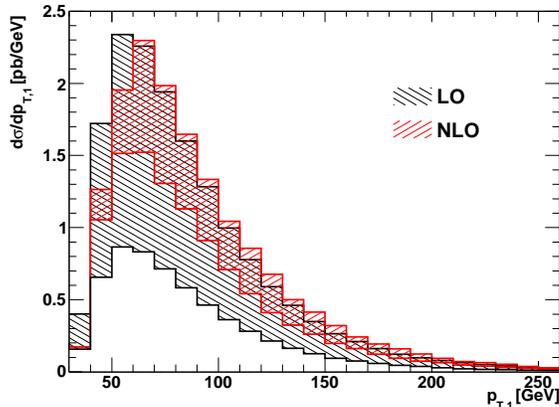
FIG. 3. p_T distribution of the hardest jet. The error bands are defined as in Figure 2.

CONCLUSIONS

We have calculated the next-to-leading order QCD corrections to the production of two bottom-antibottom quark pairs at the LHC. This calculation has been implemented in a highly automated framework for the computation of NLO QCD corrections (the `golem-2.0` framework) which is based on a Feynman diagrammatic approach for the evaluation of virtual corrections implemented in the SAMURAI and OneLOop packages, interfaced to the Madgraph/Madevent and MadDipole programs for the evaluation of the leading-order and dipole subtraction contributions and the phase space integration.

The inclusion of the NLO corrections leads to a significant reduction of the uncertainties due to unphysical scale dependence of the LO result, while enhancing the cross section by 50% for our central scale choice. Furthermore, we have shown that the radiative corrections lead to changes in the overall shape of the distributions, which cannot be accounted for in a reliable way by a simple rescaling of the leading order predictions.

This reduced theoretical uncertainty improves the prospects for the use of the $b\bar{b}b\bar{b}$ channel in searches of Higgs bosons in various extensions of the standard model like SUSY, two Higgs doublet models or hidden valley models.

This paper is dedicated to the memory of our friend Thomas Binoth who initiated this project and has always been a driving force in our collaboration.

[1] E. Richter-Was, Int. J. Mod. Phys. A **13**, 1371 (Apr 1996).

[2] E. Richter-Was and D. Froidevaux, Z.Phys. **C76**, 665 (1997), arXiv:hep-ph/9708455 [hep-ph].

[3] J. Dai, J. Gunion, and R. Vega, Phys.Lett. **B371**, 71 (1996), arXiv:hep-ph/9511319 [hep-ph].

[4] J. Dai, J. Gunion, and R. Vega, Phys.Lett. **B387**, 801 (1996), arXiv:hep-ph/9607379 [hep-ph].

[5] Z. Bern *et al.* (NLO Multileg Working Group)(2008), arXiv:0803.0494 [hep-ph].

[6] M. J. Strassler and K. M. Zurek, Phys. Lett. **B651**, 374 (2007), arXiv:hep-ph/0604261.

[7] R. Lafaye, . Miller, D.J., M. Muhlleitner, and S. Moretti(2000), arXiv:hep-ph/0002238 [hep-ph].

[8] T. Binoth, N. Greiner, A. Guffanti, J. Reuter, J.-P. Guillet, *et al.*, Phys.Lett. **B685**, 293 (2010), arXiv:0910.4379 [hep-ph].

[9] T. Stelzer and W. Long, Comput.Phys.Commun. **81**, 357 (1994), arXiv:hep-ph/9401258 [hep-ph].

[10] S. Catani and M. Seymour, Nucl.Phys. **B485**, 291 (1997), arXiv:hep-ph/9605323 [hep-ph].

[11] Z. Nagy and Z. Trocsanyi, Phys. Rev. **D59**, 014020 (1999), arXiv:hep-ph/9806317.

[12] Z. Nagy, Phys. Rev. **D68**, 094002 (2003), arXiv:hep-ph/0307268.

[13] R. Frederix, T. Gehrmann, and N. Greiner, JHEP **0809**, 122 (2008), arXiv:0808.2128 [hep-ph].

[14] R. Frederix, T. Gehrmann, and N. Greiner, JHEP **1006**, 086 (2010), arXiv:1004.2905 [hep-ph].

[15] G. Cullen, N. Greiner, G. Heinrich, G. Luisoni, P. Mastrolia, G. Ossola, T. Reiter, and F. Tramontano(work in preparation).

[16] T. Binoth, A. Guffanti, J.-P. Guillet, G. Heinrich, S. Karg, *et al.*, Nucl.Phys.Proc.Suppl. **183**, 91 (2008), arXiv:0807.0605 [hep-ph].

[17] T. Reiter(2009), arXiv:0903.0947 [hep-ph].

[18] T. Reiter(2009), arXiv:0903.4648 [hep-ph].

[19] P. Nogueira, J.Comput.Phys. **105**, 279 (1993).

[20] J. Vermaseren(2000), arXiv:math-ph/0010025 [math-ph].

[21] G. Cullen, M. Koch-Janusz, and T. Reiter, to appear in Comput.Phys.Commun.(2010), arXiv:1008.0803 [hep-ph].

[22] T. Reiter, Comput.Phys.Commun. **181**, 1301 (2010), arXiv:0907.3714 [hep-ph].

[23] P. Mastrolia, G. Ossola, T. Reiter, and F. Tramontano, JHEP **1008**, 080 (2010), arXiv:1006.0710 [hep-ph].

[24] G. Heinrich, G. Ossola, T. Reiter, and F. Tramontano, JHEP **1010**, 105 (2010), arXiv:1008.2441 [hep-ph].

[25] T. Binoth, J.-P. Guillet, G. Heinrich, E. Pilon, and T. Reiter, Comput.Phys.Commun. **180**, 2317 (2009), arXiv:0810.0992 [hep-ph].

[26] G. Cullen, J.-P. Guillet, G. Heinrich, T. Kleinschmidt, E. Pilon, *et al.*, to appear in Comput.Phys.Commun.(2011), arXiv:1101.5595 [hep-ph].

[27] A. van Hameren(2010), arXiv:1007.4716 [hep-ph].

[28] F. Maltoni and T. Stelzer, JHEP **0302**, 027 (2003), arXiv:hep-ph/0208156 [hep-ph].

[29] M. Moretti, T. Ohl, and J. Reuter(2001), arXiv:hep-ph/0102195.

[30] W. Kilian, T. Ohl, and J. Reuter(2007), arXiv:0708.4233 [hep-ph].

[31] A. Cafarella, C. G. Papadopoulos, and M. Worek, Comput. Phys. Commun. **180**, 1941 (2009), arXiv:0710.2427 [hep-ph].

[32] M. Czakon, C. Papadopoulos, and M. Worek, JHEP **0908**, 085 (2009), arXiv:0905.0883 [hep-ph].

[33] A. van Hameren, C. G. Papadopoulos, and R. Pittau, JHEP **09**, 106 (2009), arXiv:0903.4665 [hep-ph].

[34] G. C. Blazey, J. R. Dittmann, S. D. Ellis, V. Elvira, K. Frame, *et al.*, 47(2000), arXiv:hep-ex/0005012 [hep-ex].

[35] J. Pumplin, D. Stump, J. Huston, H. Lai, P. M. Nadolsky, *et al.*, JHEP **0207**, 012 (2002), arXiv:hep-ph/0201195 [hep-ph].